Special Issue Article

Journal of PeptideScience

Received: 1 October 2012 Revised: 23 November 2012 Accepted: 26 November 2012 Published online in Wiley Online Library: 16 January 2013

(wileyonlinelibrary.com) DOI 10.1002/psc.2477

Quantifying molecular partition of cell-penetrating peptide–cargo supramolecular complexes into lipid membranes: optimizing peptide-based drug delivery systems‡

João Miguel Freire,[a] Ana Salomé Veiga,[a] Beatriz G. de la Torre,[b] David Andreu[b] and Miguel A. R. B. Castanho[a]*

One of the major challenges in the drug development process is biodistribution across epithelia and intracellular drug targeting. Cellular membrane heterogeneity is one of the major drawbacks in developing efficient and sustainable drug delivery systems, which brings the need to study their interaction with lipids in order to unravel their mechanisms of action and improve their delivery capacities. Cell penetrating peptides (CPPs) are able to translocate almost any cell membrane carrying cargo molecules. However, different CPP use different entry mechanisms, which are often concentration-dependent and cargo-dependent. Being able to quantify the lipid affinity of CPP is of obvious importance and can be achieved by studying the partition extent of CPP into lipid bilayers. The partition constant (K_p) reflects the lipid–water partition extent. However, all currently available methodologies are only suitable to determine the partition of single molecules into lipid membranes or entities, being unsuitable to determine the partition of bimolecular or higher order supramolecular complexes. We derived and tested a mathematical model to determine the K_p of supramolecular CPP-cargo complexes from fluorescence spectroscopy data, using DNA oligomers as a model cargo. As a proof-of-concept example, the partition extent of two new membrane active peptides derived from dengue virus capsid protein (DENV C protein) with potential CPP properties, in both scenarios (free peptide and complexed with a molecular cargo), were tested. We were able to identify the lipid affinity of these CPP:DNA complexes, thus gaining valuable insights into better CPP formulations. Copyright © 2013 European Peptide Society and John Wiley & Sons, Ltd.

Keywords: drug delivery; cell penetrating peptide; membrane interaction; spectroscopy; fluorescence

Introduction

One of the major challenges in drug development process is the biodistribution across epithelia and intracellular drug targeting [1,2]. Target specificity is also of utmost importance to improved efficacy with less adverse off-target effects and resistance to treatment [3]. Over the years, several drug delivery systems have been developed and optimized [4] to improve biodistribution and increase target specificity. A wide variety of cargos with therapeutic application have been successfully delivered by CPP into various types of cells for the treatment of multiple diseases [5]. Typically, these peptides consist of 6–30 amino acid sequences, usually rich in cationic residues, along with hydrophobic or amphipathic ones [2,6,7]. Within these general traits, CPP displays a variety of structural and biochemical properties [2,7], yet share the ability to translocate virtually every cell membrane, thus providing a perfect template for designing effective intracellular deliver agents. In tune with this, a growing number of CPP studies over the last 20 years [2,8] is devoted to drug delivery issues (Figure 1(A)), particularly the translocation of cargos such as small RNA/DNA, plasmids for cell transfection, antibodies and nanoparticles. The mechanism underlying cellular translocation has been intensively studied, mainly using the HIV-1 transcriptional activator (Tat) [9] and penetratin from the *Antennapedia* homeodomain of Drosophila [2,6], and has shown to depend on CPP concentration, peptide-to-cell ratio, type of cargo conjugated, and chemical nature of peptide–cargo conjugation [10].

Cellular membrane heterogeneity is one of the major bottlenecks in developing efficient and sustainable drug delivery systems, yet may be an advantage for target specific therapies [3]. Because CPP exert their effects primarily at the cell membrane level, studying their interactions with lipids is crucial to ascertain their mechanism of action [11,12].

* *Correspondence to: Miguel A. R. B. Castanho, Instituto de Medicina Molecular, Faculdade de Medicina da Universidade de Lisboa, Av. Prof. Egas Moniz, 1649–028 Lisboa, Portugal. E-mail: macastanho@fm.ul.pt*

‡ *Special issue devoted to contributions presented at the 13th Naples Workshop on Bioactive Peptides, June 7–10, 2012, Naples.*

a *Instituto de Medicina Molecular, University of Lisbon, Physical Biochemistry Unit, Lisbon, Portugal*

b *Department of Experimental and Health Sciences, Pompeu Fabra University, Barcelona Biomedical Research Park, E-08003 Barcelona, Spain*

Abbreviations used: *CPP, Cell penetrating peptide; DENV, Dengue virus; C protein, Capsid protein.; RBA, RNA Binding Sequence; MBS, Membrane binding Sequence.*

Journal of PeptideScience

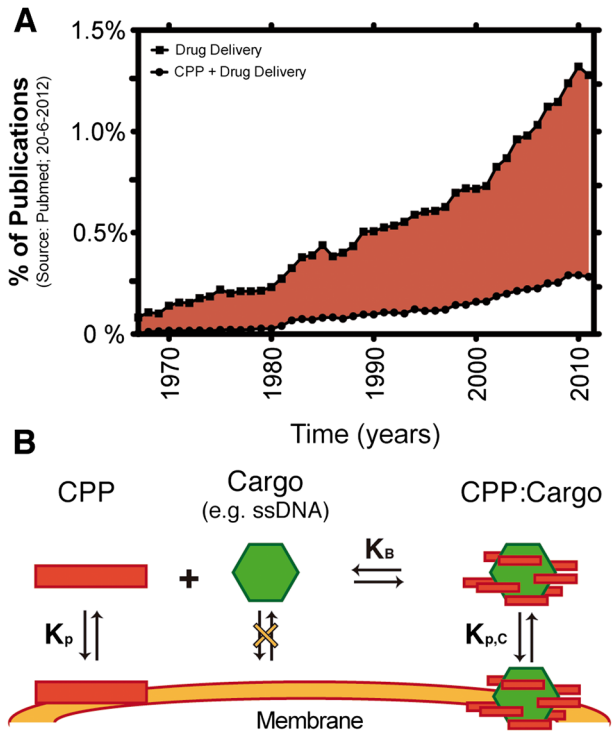

Figure 1. (A) Research on CPP as drug delivery agents has increasing importance. Chronographical analysis of drug delivery related publications at the PubMed online database [Query: Drug Delivery; assessed at 20-6-2012 (squares)] and CPP-mediated drug delivery (circles) (Query: CPP + Drug Delivery; assessed at 20-6-2012). Publications were normalized to the total Medline biomedical publications at each year and are represented as the number of papers per 100 publications. (Analysis was obtained with the web-tool: *Medline trend: automated yearly statistics of PubMed results for any query, 2004. Alexandru Dan Corlan*. http://dan.corlan.net/medline-trend.html). (B) Schematic representation of the double partition equilibrium of the CPP and CPP–cargo molecules between the aqueous and lipid membrane. Concomitant double partition (involving both free CPP, K_p, and the CPP–cargo complexes, $K_{P,C}$) and aqueous binding equilibrium between CPP and the cargo, responsible for the complex formation, K_b, needs to be considered. This methodology allows determination of the membrane partition constant ($K_{P,C}$) of the CPP–cargo complex.

The molecular lipid/water partition extent, expressed by the partition constants (K_p), is a useful parameter to establish the 'lipid affinity' of peptides [13–15]. Partition events can be studied using liposomes and other vesicular lipid models [14,16] that are useful because they mimic adequately several cell membrane properties in a wide range of interactions. However, current available methodologies only quantify the partition of single molecular entities into lipid membranes, being unable to determine the partition constants of multi-equilibrium systems in which CPP forms supramolecular complexes. In this work, we have derived and validated a mathematical methodology to determine the K_p of supramolecular CPP-Cargo (e.g. DNA) DNA complexes, $K_{p,C}$, from fluorescence spectroscopy data. As a proof-of-concept example, the partition extent of two new membrane active peptides derived from dengue virus capsid protein (DENV C protein) with potential CPP properties, in both scenarios (free peptide and complexed with a molecular cargo), has been tested. Both the partition constant of the unbound CPP, K_p, and CPP-cargo, $K_{p,C}$ are retrieved. The referred peptides are currently being extensively tested for their CPP activity.

Dengue virus C protein may be assigned to the new CPP family designated as supercharged proteins, being a potential CPP itself. However, being a homodimer [17,18] and having 200 amino acid residues in total, future applications with this protein would be limited. We designed DENV C protein-derived peptides with cell translocation ability to serve as CPP sequence templates. From the three-dimensional structure of DENV C protein [18], one highly positively charged sequence, putatively assigned to RNA-binding [18] and one hydrophobic conserved region putatively assigned to membrane interactions [17] (RBS-RNA Binding Sequence; and MBS-Membrane Binding Sequences domains, respectively) were defined. Two synthetic peptides, pepR (LKRWGTIKKSKAINVLRGFRKEIGRMLNILNRRRR – residues 67–100 of DENV-2 C protein [18]) and pepM (KLFMALVAFLRFLTIPPTA-GILKRWGTI – residues 45–72 of DENV-2 C protein), respectively, containing the RBS and the MBS domains, were synthesized. Studies with pepR have already reported its antimicrobial activity [19]. Given the close sequence and structural similarities between CPP and antimicrobial peptides [2,6,20,21], it is not surprising that pepR scores in both categories.

Materials and Methods

Theoretical Background

In this work, the mathematical methodology to determine the partition constant of supramolecular complexes to lipid membranes is described in detail and tested with two DENV C protein-derived CPP carrying a nucleic acid cargo. The extent of pepR and pepM (and respective ssDNA complexes) partition into model membranes (zwitterionic and anionic large unilamellar vesicles (LUV)) was evaluated by fluorescence spectroscopy.

The mathematical model

Solute partition is the distribution of a solute between two immiscible phases, and this concept can be adapted to address the interactions of membrane active molecules with lipid bilayers. In this work, the concept will be extended to consider supramolecular complexes interacting with membranes. The definition and quantification of a partition constant of a solute that distributes between an aqueous and a lipid phase, K_p, are addressed and well documented in the literature [13,14,22]. In membrane-active peptides containing tryptophan or tyrosine amino acid residues, its quantification can be achieved by monitoring the intrinsic fluorescence emission of those residues when aqueous solutions of peptides are titrated with lipid vesicles. In the present case, the natural peptide's fluorescence due to the Trp residue was used to perform data analysis.

For a chosen spectroscopic signal associated to a certain sample, there is a balance between the signals from the molecules located in each phase (aqueous and lipid). This balance relies on the fractional distribution of the molecules between aqueous and lipid media, i.e. on the K_p. K_p definition has thermodynamic backgrounds [14,15]. The equilibrium constant between these two immiscible phases is described by

$$K_p = \frac{\frac{n_{S,L}}{V_L}}{\frac{n_{S,W}}{V_W}} = \frac{[\text{Solute}]_L}{[\text{Solute}]_W} \quad (1)$$

where $n_{S,W}$ and $n_{S,L}$ are, respectively, the moles of solute in the water and lipid environment and V_i are the volumes of each phase ($i = W$, aqueous phase; $i = L$, lipid phase).

In the absence of phenomena other than partition (such as saturation or self-quenching), the measured spectroscopic signal is described by Eqn (2) [13,14]. The spectroscopic parameter may be any additive signal such as electronic absorbance, fluorescence intensity, fluorescence lifetime-weighted quantum yield, steady-state fluorescence anisotropy [23], or circular dichroism data.

$$\frac{I}{I_W} = \frac{1 + K_P \gamma_L \frac{I_L}{I_W}[L]}{K_P \gamma_L [L]} \tag{2}$$

I_W and I_L are the fluorescence intensities with all the fluorophore in aqueous solution or in lipid, respectively, γ_L is the molar volume of lipid, and $[L]$ is its concentration [14]; the γ_L used was $0.763\,dm^3\,mol^{-1}$ for vesicles containing 1-palmitoyl-2-oleoyl-*sn*-glycero-3-phosphocholine (POPC) [24].

A novel mathematical model was derived, accounting for simultaneous partition of both the free and complexed peptides (Figure 1(B)), which are in equilibrium with the free ssDNA molecules. This novel mathematical formalism is an extension of the described partition model [14] with other chemical equilibrium equations [25,26].

The model considers a membrane-active molecule (e.g. CPP) that associates to other molecule (the cargo). In the presence of a lipid membrane, both the free peptide and the supramolecular complex interact with lipids, a condition necessary for intracellular delivery of the cargo by the CPP. When a peptide is in solution with a cargo such as oligonucleotides in the presence of membranes, several biochemical equilibria occur. In the aqueous environment, there is free peptide (PW) and peptide associated to the cargo (e.g. oligonucleotide – PD), and both may insert or adsorb with the lipid membrane, forming the species PL (free peptide in the membrane) or PDL (peptide-oligonucleotide aggregate in the membrane).

Assuming that the peptide is fluorescent, the fluorescence signal acquired from the sample is the sum of the fluorescence from each species in solution:

$$I = I_{PW}X_{PW} + I_{PD}X_{PD} + I_{PL}X_{PL} + I_{PDL}X_{PDL} \tag{3}$$

where I_i are the total fluorescence intensity that would be detected if all peptides were in environment i (W, noncomplexed peptide in aqueous solution; L, noncomplexed in the lipid bilayer; CW, complexed with ssDNA in aqueous solution; CL, complexed with ssDNA in the lipid bilayer).

For the sake of simplicity and feasibility, a 1:1 stoichiometry between the peptide and the molecule to which it associates is considered. It is also assumed that the molecule that interacts with the peptide (e.g., oligonucleotide) is nonfluorescent at the wavelength of excitation and does not interact with the lipid membrane in its free form, which is the usual situation for a hydrophilic cargo. Therefore, the interaction with the lipid bilayer is assumed to be exclusively because of lipid–peptide interactions. Then, two different possibilities have to be considered: (i) if the fluorescence emission of the peptide is not quenched by the cargo in the complex, a formalism similar to what is used by Veiga *et al.* [26] can be considered; (ii) if the peptide fluorescence emission is quenched by the cargo or self-quenching phenomena may occur, therefore, the formalism by Veiga *et al.* has to be adapted.

(A) If there is no quenching or other spectroscopic interference on the CPP–cargo binding

$$I_{PW} = I_{PD} \text{ and } I_{PL} = I_{PDL} \tag{4}$$

Equation (3) can be rearranged as follows:

$$I = I_{PW}(X_{PW} + X_{PD}) + I_{PL}(X_{PL} + X_{PDL}) \tag{5}$$

Considering that the lipid fraction of peptide is

$$\Xi_L = X_{PL} + X_{PDL} \tag{6}$$

(Ξ_L is the sum of both CPP and CPP:cargo molar fraction in the lipid membrane) and the aqueous fraction is

$$X_{PW} + X_{PD} = 1 - \Xi_L \tag{7}$$

To compare data acquired in different occasions and between different CPP and CPP–cargo, the normalized fluorescence signal is

$$\frac{I}{I_{PW}} = 1 + \left(1 - \frac{I_{PL}}{I_{PW}}\right)\Xi_L \tag{8}$$

The molar fraction of the free peptide bound to the membrane, X_{PL}, is

$$X_{PL} = \frac{n_{PL}}{n_{PL} + n_{PD} + n_{PW} + n_{PDL}} \tag{9}$$

Considering the partition and CPP–cargo binding equilibria:

$$K_b[D] = \frac{n_{PD}}{n_{PW}} \text{ and } K_P = \frac{[P]_L}{[P]_W} \Leftrightarrow \frac{n_{PW}}{n_{PL}} = \frac{1}{K_P \gamma_L [L]} \tag{10}$$

(P – peptide; L – lipid; D – cargo) The molar fraction of the bound peptide free is

$$X_{PL} = \frac{1}{1 + \beta + \frac{1 + K_B[D]}{K_P \gamma_L [L]}} \tag{11}$$

where β represents the ratio between free and complexed peptide that interact with the membrane.

$$\beta = \frac{n_{PDL}}{n_{PL}} \tag{12}$$

This parameter gives us information on which molecular species (CPP or CPP–cargo) interacts more extensively with the lipid membrane.

Using the same methodology applied before for X_{PL}, the fraction of peptide involved in the CPP–cargo complexes that interacts with the membrane, X_{PDL}, is

$$X_{PDL} = \frac{1}{1 + \frac{1}{\beta} + \frac{1}{K_{P,C}\gamma_L[L]}\left(1 + \frac{1}{K_B[D]}\right)} \tag{13}$$

Substituting X_{PL} and X_{PDL} in Eqn (8) by equations (11) and (13), respectively, one can determine the partition constant of the

Journal of PeptideScience

complex ($K_{p,C}$), as well as the complex-to-free peptide molar ratio in the membrane by means of β. In principle, K_B (apparent CPP–cargo binding equilibrium constant) can be determined. However, if parallel experiments, such as isothermal calorimetry, are used to determine K_B independently, then nonlinear fitting of Eqn (8) enables to determine $K_{p,C}$ and β very accurately.

(B) If the CPP signal is perturbed upon interaction with the cargo molecule (e.g. the peptide's fluorescence is quenched), then Eqn (3) is no longer valid. In this case,

$$I_{PD} = \alpha_W I_{PW} \tag{14}$$

with α reflecting the magnitude in the variation of the peptide fluorescence quantum yield. Assuming that the quenching efficiency is not influenced by the changes in the environment polarity:

$$\alpha_W \equiv \alpha_L \equiv \alpha \tag{15}$$

$$I_{PDL} = \alpha_L I_{PL} \tag{16}$$

The total fluorescence emission intensity (Eqn (3)) can be rewritten as

$$I = I_{PW}(X_{PW} + \alpha X_{PD}) + I_{PL}(X_{PL} + \alpha X_{PDL}) \tag{17}$$

and can be rearranged as

$$\frac{I}{I_{PW}} = 1 + X_{PD}(\alpha - 1) - \Xi_L + \frac{I_{PL}}{I_{PW}}(X_{PL} + \alpha X_{PDL}) \tag{18}$$

because

$$X_{PW} + \alpha X_{PD} = 1 + X_{PD}(\alpha - 1) - \Xi_L \tag{19}$$

The molar fraction of the CPP:cargo complex, X_{PD}, in water has now to be determined. The fraction of aqueous free peptide is

$$X_{PW} = 1 - (X_{PD} + \Xi_L) \tag{20}$$

The cargo concentration is described by

$$[D] = [D]_{\text{total}} - [P]_{\text{total}}(X_{PD} + \Xi_L) \tag{21}$$

and the free peptide fraction is

$$X_P = \frac{1}{1 + K_b\left([D]_{\text{total}} - [P]_{\text{total}}(X_{PD} + \Xi_L)\right)} \tag{22}$$

Solving Eqn (21) in order to X_{PD}, a polynomial quadratic equation, $ax^2 + bx + c = 0$, is obtained, yielding

$$X_{PD} = \frac{-b \pm \sqrt{b^2 - 4ac}}{2a} \tag{23}$$

where

$$a = K_b[P]_{\text{total}}$$
$$b = K_b\left(\frac{1}{K_b} + [p]_{\text{total}} + [D]_{\text{total}} + 2\Xi_L[P]_{\text{total}}\right)$$
$$c = \left(\Xi_L K_b\left([P]_{\text{total}}\Xi_L - [P]_{\text{total}} - [D]_{\text{total}} - \frac{1}{K_b}\right) + K_b[D]_{\text{total}}\right)$$

One can obtain the fraction of supramolecular complex, X_{PD}. By the nonlinear fitting of Eqn (18), using Eqns (11), (13), and (22) for the X_{PL}, X_{PDL}, and X_{PD} values, respectively, it is possible to determine the lipid partition constant of CPP–cargo complexes, $K_{P,C}$.

By analyzing the boundaries of either Eqn (8) or (18), one can optimize experimental conditions to simplify the mathematical data analysis formalism.

1) When $[L] \to 0$.

With no lipid membranes in the system, only the aqueous equilibrium between the CPP and the cargo occurs. In this limit, $X_{PDL} = 0$ and $X_{PL} = 0$. The system is transformed in the equilibrium described by Ribeiro *et al.* [25], represented by

$$X_{PD}^2 K_b[P]_{\text{total}} - X_{PD}\left(1 + K_b[D]_{\text{total}} + K_b[P]_{\text{total}}\right) + K_b[D]_{\text{total}} = 0 \tag{24}$$

2) When $[D] \to 0$ or $K_D = 0$.

This is the standard partition situation described elsewhere [14]. There is only lipid, water, and peptide in the system, thus $X_{PDL} = 0$ and $X_{PD} = 0$. The system becomes an equilibrium that is described by

$$\frac{I}{I_{PW}} = \frac{1 + K_P\gamma_L[L]\frac{I_{PL}}{I_{PW}}}{1 + K_P\gamma_L[L]} \tag{25}$$

3) When $[L] \to \infty$.

This would be the mathematical limit in which all the peptides, either free or complexed with the oligonucleotides, are inserted and interacting with the lipid bilayer. Therefore,

$$1 = \Xi_L = X_{PL} + X_{PDL} \tag{26}$$

where

$$X_{PL} = \frac{1}{1 + \beta} \text{ and } X_{PDL} = \frac{1}{1 + \frac{1}{\beta}} \tag{27}$$

Equations (7) and (17) would become, respectively,

$$\frac{I}{I_{PW}} = \frac{I_{PL}}{I_{PW}}\left(\frac{1 + \alpha\beta}{1 + \beta}\right) \tag{28}$$

and

$$\frac{I}{I_{PW}} = \frac{I_{PL}}{I_{PW}} \tag{29}$$

4) When $K_B \to +\infty$, where $X_{PDL} + X_{PD} = 1$ and $X_{PW} \approx X_{PL} \approx 0$.

In this case, it is assumed that all the molecular species in solution are CPP–cargo supramolecular complexes. No free peptide is available to interact with the lipid bilayer; therefore, only the complexes may interact with the lipid membrane. The equations can then be rearranged, and a simplified equation is obtained similar to the standard partition model but valid for peptide–cargo partition and accounting for eventual quenching effects due to complexation (α parameter):

$$\frac{I}{I_{PW}} = \alpha\left(\frac{1 + k_{P,C}\gamma_L[L]\frac{I_{PL}}{I_{PW}}}{1 + K_{P,C}\gamma_L[L]}\right) \tag{30}$$

where α is equal to I_{PD}/I_{PW} ($\alpha = 1$ if there is no quenching). Förster resonance energy transfer (FRET) and dynamic light scattering (DLS) experiments, for instance, can be used to follow the association of CPP and cargo molecules so that experimental

conditions where no free peptide existence are selected. These selected experimental conditions may be experimentally used to determine the partition constant of the supramolecular complexes, $K_{p,C}$, by fitting the data with Eqn (30).

The simple and straightforward Eqn (30) is a tool to compare newly designed and improved CPP as drug carriers and guide drug developers towards CPP optimization in lipid membrane binding. This novel mathematical lipid partition model may serve as a good screening tool for optimization of simultaneously CPP–cargo–lipid membrane interactions, which are major requisites for a proper drug delivery system with potential biomedical application. The optimization of CPP has been largely based on empirical approaches and almost entirely based on rather meaningless interaction of free CPP with lipids, in the absence of cargo. It is expected that the methodology here derived contribute to a more effective and rational design of cellular entry vectors.

Chemicals

Fmoc-protected amino acids were obtained from Senn Chemicals (Dielsdorf, Switzerland) and Fmoc-Rink-amide (MBHA) resin from Novabiochem (Läufelfingen, Switzerland). 2-(1*H*-benzotriazol-1-yl)-1,1,3,3-tetramethyluronium hexafluorophosphate (HBTU) and *N*-hydroxybenzotriazole (HOBt) were from PCAS Biomatrix (Saint Jean sur Richelieu, Quebec, Canada). HPLC-grade acetonitrile and peptide synthesis-grade *N*,*N*-dimethylformamide (DMF), dichloromethane, *N*,*N*-diisopropylethylamine (DIEA), and trifluoroacetic acid (TFA) were from Carlo Erba-SDS (Sabadell, Spain). The 15 nucleotide ssDNA primer (ACG TGC TGA GCC TAC) used as molecular cargo model and a version labeled with the fluorescent dye Alexa-488 (ssDNA-Alexa488) were obtained from Molecular Probes/Invitrogen (Life Technologies, Carlsbad, CA, USA). Dipalmitoylphosphatidylcholine, POPC, and 1-palmitoyl-2-oleoyl-*sn*-glycero-3-(phospho-*rac*-(1-glycerol)) (POPG) were purchased from Avanti Polar Lipids (Alabaster, Alabama, USA). 4-(2-Hydroxyethyl)-1-piperazineethanesulfonic acid, NaCl, Triton X-100, 5-doxyl-stearic acid (5-NS), and 16-doxyl-stearic acid (16-NS) were acquired from Sigma-Aldrich (St. Louis, Missouri, USA). All other reagents were of the highest quality available commercially.

CPP synthesis – pepR and pepM

Both pepR (LKRWGTIKKSKAINVLRGFRKEIGRMLNILNRRRR – residues 67–100 of DENV-2 C protein) and pepM (KLFMALVAFLRFLTIPPTAGILKRWGTI – residues 45–72 of DENV-2 C protein), as well as their N-terminal rhodamine B-labeled versions, were prepared by solid phase synthesis methods [27] in an ABI433 peptide synthesizer (Applied Biosystems) running standard Fmoc (FastMoc) protocols at 0.1 mmol scale on Fmoc-Rink-amide MBHA resin, as previously described [19] (Table 1). Eightfold excess of Fmoc-L-amino acids and HBTU/HOBt, in the presence of double that molar amount of DIEA, was used for the coupling steps, with DMF as solvent. All side-chain functions were protected with TFA labile groups. Rhodamine B was coupled manually, with tenfold excess, in the presence of an equivalent amount of DIPCDI in DMF. Peptide was precipitated by the addition of chilled diethyl ether, taken up in aqueous acetic acid (10% v/v), and lyophilized. Analytical reversed-phase HPLC was performed on C_8 and C_{18} columns (4.6 × 50 mm, 3 μm, Phenomenex) in a model LC-2010A system (Shimadzu). Solvent A was 0.045% (v/v) TFA in water, and solvent B 0.036% (v/v) TFA in acetonitrile. Elution was carried out with linear gradients of solvent B into solvent A over 15 min at 1 mL min^{-1} flow rate, with UV detection at 220 nm, 30 °C. Preparative HPLC was performed on C_8 column (21.2 × 250 mm, 10 μm, Phenomenex) in a Shimadzu LC-8A instrument. In this case, solvents A and B were 0.1% TFA (v/v) in water and acetonitrile, respectively, and elution was again with linear gradients of solvent B into A over 30 min, at 25 mL/min flow rate, with UV detection at 220 nm. Preparative fractions of purity ≥90% by analytical HPLC were pooled and lyophilized. The HPLC-purified peptides were characterized for identity by MALDI-TOF mass spectrometry in a Voyager DE-STR instrument (Applied Biosystems, Foster City, California, USA), operating in the reflector mode and using α-hydroxycinnamic acid matrix (Table 1). pepR and pepM stock solutions were prepared in Milli Q Water.

Lipid vesicles preparation

Large unilamellar vesicles, typically with 100 nm diameter, were used as membrane model systems and were prepared by the extrusion protocol described elsewhere [28]. Briefly, lipid mixtures were prepared in rounded glass flasks and dried in vacuum overnight. The solution was then rehydrated and submitted to 8 freeze/thaw cycles before performing the extrusion procedure with a 100-nm pore membrane using an Avestin LiposoFast Extruder apparatus. Two lipid systems were analyzed, namely POPC and POPC:POPG (4:1).

CPP–cargo association by FRET and DLS

The interaction of CPP, pepR, and pepM, with the cargo model, an ssDNA molecule, was studied by FRET and DLS. The first reports peptide–ssDNA association at the molecular level, whereas the latter reports the formation of mixed peptide–ssDNA supramolecular aggregates.

Dynamic light scattering experiments were carried out on a Malvern Zetasizer Nano ZS (Malvern, UK) with a backscattering detection at 173°, equipped with a He-Ne laser (λ = 632.8 nm), at 25 °C (15 min of equilibration). pepR and pepM in the presence

Table 1. Sequences and chemical properties of pepM, pepR, and their fluorescent derivatives

	Sequence	Formula	MW [Da]	$[M+H^+]^a$	HPLC[b] RT (min)
pepR	LKRWGTIKKSKAINVLRGFRKEIGRMLNILNRRRR	$C_{189}H_{335}N_{69}O_{42}S_1$	4278.2	4276.4	3.8
RhB-pepR	RhB-LKRWGTIKKSKAINVLRGFRKEIGRMLNILNRRRR	$C_{217}H_{364}N_{71}O_{44}S_1$	4703.4	4704.5	6.4
pepM	KLFMALVAFLRFLTIPPTAGILKRWGTI	$C_{155}H_{250}N_{38}O_{31}S_1$	3173.9	3173.0	7.9
RhB-pepM	RhB-KLFMALVAFLRFLTIPPTAGILKRWGTI	$C_{183}H_{279}N_{40}O_{33}S_1$	3599.2	3597.2	11.0

[a]MALDI-TOF spectra recorded in a Voyager DE-STR instrument (Applied Biosystems) in the linear mode, using α-hydroxycinnamic acid matrix. In the last entry, the observed peak corresponds to the sodium adduct.

[b]Analytical RP-HPLC on C_{18} columns (4.6 × 50 mm, 3 μm, Phenomenex) using a linear 20–70% gradient of solvent B into A over 15 min, 1 mL/min flow rate, UV detection at 220 nm, 30 °C. Solvents A and B are 0.045% (v/v) TFA in water and 0.036% (v/v) TFA in acetonitrile, respectively.

Journal of PeptideScience

of the ssDNA oligonucleotide, 50 μL of 100 μM pepR or pepM, were prepared with peptide:ssDNA molar ratios at 5:1 (Figure 2 (A)). For each sample, the instrument was set to perform 15 scans, each one giving an autocorrelation curve after at least 70 measurements, with an initial equilibration time of 15 min at 25 °C. Normalized intensity autocorrelation function, average of 15 obtained, was analyzed using the CONTIN method [29,30], retrieving a distribution of diffusion coefficients (D), which can be used for the calculation of the hydrodynamic diameter (D_H) [31,32] distribution through the Stokes–Einstein (Eqn (31)) and determine the mode of the dimension of the scattered particle:

$$D + \frac{kT}{3\pi\eta D_H} \tag{31}$$

where k is the Boltzmann constant, T the absolute temperature, and η the medium viscosity. The D_H of the sample was considered from the peak with the highest scattered light intensity (i.e., the mode) in light scattering intensity distributions.

In FRET experiments, a 2 μM ssDNA-Alexa488 solution was titrated with either pepR or pepM labeled with Rhodamine B at a maximum molar peptide:ssDNA ratio of 5:1. Samples were excited at 492 nm; emission spectra were collected from 500 to 700 nm and blank corrected. FRET efficiency in the absence and presence of peptide were calculated according to [33]

$$\text{FRET efficiency} = 1 - \frac{I_i}{I_0} = \frac{R_0^6}{R_0^6 + r^6} \tag{32}$$

where I_0 and I_i are the fluorescence emission intensity at the acceptor maximum wavelength for the donor in buffer and after the addition of the concentration i of peptide, respectively.

CPP–cargo partition to lipid bilayers

Membrane partition studies were performed by successive additions of a 15-mM LUV suspension to final concentrations up to 5 mM (POPC, POPC:POPG (4:1)) to a 36 μM pepR, pepM solution. For the CPP–cargo lipid partition experiments, preassociated CPP–cargo complexes of either 36 μM of pepR or pepM and ssDNA (molar ratio of 5:1 peptide:ssDNA) were also titrated to a LUV concentration up to 5 mM.

The fluorescence lifetime decays of each experiment condition during LUV titration were obtained with a LifeSpec II equipped with an Epled-280 (laser of 275 nm with a repeating rate of 200 ns). The wavelength recording value was set at the tryptophan emission maximum (350 nm) with emission slits opened to 23 and 40 nm for pepR and pepM, respectively. A 20-ns range was used for decay acquisition using a 2048-channel system for 20 min. Instrumental response functions were generated from scatter dispersion (glycogen solution (Acros Organics, Belgium)). FAST software was used for further data analysis by using a nonlinear least-squares iterative convolution method (Edinburg

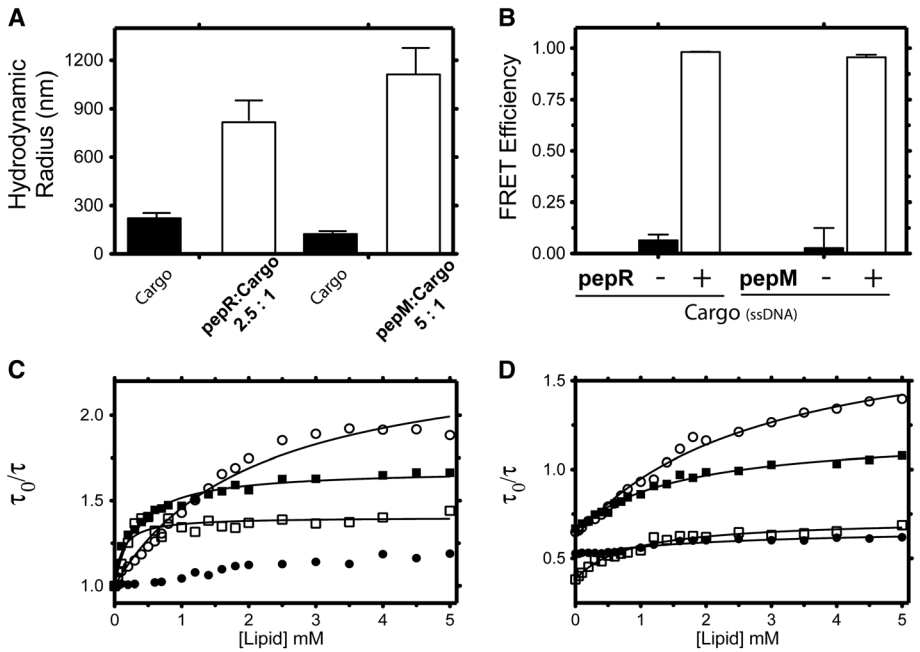

Figure 2. Application of the developed methodology using two DENV C protein-derived membrane active peptide – pepM and pepR. (A) Mode of the hydrodynamic diameter distribution histograms [31,32], obtained by dynamic light scattering spectroscopy. 100 μM pepR or pepM in the absence (black) and presence (white) of ssDNA at a peptide:ssDNA ratio of 2.5:1 (pepR) or 5:1 (pepM). Significant size distribution changes are observed after the ssDNA addition. Error bars show the SD of three independent experiments. (B) Association between pepR and pepM and the molecular cargo (ssDNA), determined by FRET [36] at pH 7.4. Energy transfer between the cargo (ssDNA labeled with alexa-488 – donor) and pepR or pepM (labeled with Rhdamine-B acceptor). pepR or pepM at a peptide:cargo molar ratio of 4:1 was added to a 2 μM ssDNA solution (white). Free ssDNA is represented by the black bars. Energy transfer from the ssDNa dye to the CPP dye was observed indicating association between both molecular entities. (C) and (D) pepR (circles) and pepM (squares) (C) and their respective ssDNA complexes (D) lipid partition extent studies. A 36 μM solution of pepM or pepR and pepM-ssDNA or pepR-ssDNA (4:1 molar ratio) solution was titrated with LUV of POPC (■, pepM and ●, pepR) or POPC:POPG (4:1, □ – pepM, ○ – pepR) at pH 7.4. Fluorescence lifetime decays were acquired with an excitation wavelength of 280 nm, and the average fluorescence lifetimes acquired were normalized for the value obtained in the absence of LUV. Eqns (2) and (30) were used to fit the data to obtain the partition constants, K_p for the CPP and $K_{p,C}$ for the CPP–cargo, respectively (Table 1).

Instruments, UK). Each decay was considered a weighted sum of exponentials:

$$I(t) = \sum \alpha_i e^{\frac{-t}{\tau_i}} \quad (33)$$

where α_i is the weighting pre-exponential factor in the multiexponential intensity decay, t is time, and τ_i is the fluorescence life-time [33]. The goodness of the fit was judged from the global residuals distribution and the global χ^2 values (decay plots with $0.99 < \chi^2 < 1.1$ were selected). The Trp fluorescence decay was described by the sum of three exponentials [16]. The average lifetime, $\langle\tau\rangle$, and the fluorescence lifetime averaged by the pre-exponential factors, τ_α, were determined according to

$$\langle\tau\rangle = \frac{\sum \alpha_i \tau_i^2}{\sum \alpha_i \tau_i^2} \quad (34)$$

$$\tau_\alpha = \frac{\sum \alpha_i \tau_i}{\sum \alpha_i} \quad (35)$$

By substituting the fluorescence intensity parameters at Eqns (3) and (31) by the average fluorescence lifetime values, one can use time-resolved fluorescence data to evaluate the partition extent of our system towards lipid membranes. This approach is feasible because of the additive properties of the pre-exponential averaged fluorescence lifetime. With this parameter, the relationship $I_0/I = \langle\tau\rangle_0/\langle\tau\rangle$ is valid, thus leading to the use of same straightforward partition formalism previously stated for steady-state fluorescence for fluorescence lifetime data. However, if one uses steady state fluorescence data, corrections regarding light scattering or other spectroscopic artifacts induced by the addition of lipid vesicles should be applied to the fluorescence intensity spectra according to Ladokhin *et al.* [34].

Results and Discussion

To test the previously described methodology, we first evaluated the association between both CPP (pepR and pepM) with the cargo (we used an ssDNA molecule as cargo model). The CPP–cargo complex formation was studied by FRET (Figure 2(A)) and DLS (Figure 2(B)). The first reports peptide–ssDNA association at the molecular level, whereas the latter reports the formation of mixed peptide–ssDNA supramolecular aggregates. Both results (Figure 2(A) and (B)) reveal that pepM and pepR are able to interact with ssDNA forming supramolecular aggregates. The size of the scattering particles increased in the presence of ssDNA, which indicates that pepR and pepM form supramolecular complexes with the ssDNA. FRET experiments support DLS observations by observing energy transfer between the fluorescent dye of the cargo (Alexa 488) and the peptide label (Rhodamine B) at a molar ratio of 5:1 (CPP–cargo). Therefore, one can proceed to test whether these supramolecular complexes pepR-ssDNA and pepM-ssDNA are able to interact with lipid membranes, a major requisite to further internalize into the lipid bilayer.

The CPP–lipid interaction was evaluated by membrane partition studies using LUV as lipid membrane models with lipid mixtures of POPC and POPC:POPG (4:1). Time resolved fluorescence data was used instead of steady-state fluorescence. Using fluorescence life-time data, a more precise information about the intra- and inter-molecular interaction is achieved [14,16]. The Trp fluorescence decay was then described by the sum of three exponentials [16]. By applying the nonlinear fit of either Eqns (2) or (30) to the average fluorescence lifetime values, one can use time-resolved fluorescence data to evaluate the partition extent of the CPP and CPP–cargo complexes toward lipid membranes (Figure 2(C) and (D) and Table 2). With this evaluation, one can analyze each CPP preferential lipid membrane composition as well as which CPP is able to adsorb more at the bilayer with its cargo. The higher the affinity of the CPP–cargo complex to the membrane, the more efficient membrane translocation occur [13,15,35]. The affinity of these complexes to lipid membranes and the preferential lipid composition of the membrane to enhance this interaction was quantified for several lipid mixtures in order to illustrate the application of our newly developed model (Figure 2 and Table 2). We were able to determine the partition constant for the CPP–cargo (pepR–ssDNA and pepM–ssDNA) complexes. The partition curves for both free pepR and pepM (Figure 2(C)) and each correspondent peptide:ssDNA complex (Figure 2(D)) for POPC and POPC:POPG (4:1) are shown. Table 2 resumes the partition constants for each system. The results show that both peptides prefer liquid-disordered lipids enriched with negatively charged lipids. pepM also partitions toward POPC fluid membranes; however, the increase in POPG content in the membranes increased the partition constant, K_p. As for pepR, a percentage of negatively charged lipids is required for peptide–lipid interaction, as no partition to POPC membranes was detected. These lipid mixtures were further used to evaluate the interaction of the CPP–cargo complexes with lipid membranes (Figure 2(D) and Table 2). Table 2 revealed that both pepR:ssDNA and pepM:ssDNA complexes are able to interact with lipid membranes. It should be stressed that pepR itself did not interact with POPC membranes; however, in its complexed form with the ssDNA

Table 2. pepR, pepM, and respective ssDNA complexes partition to lipid vesicles

Partition constant, K_p ($\times 10^3$)

	POPC			POPC:POPG (4:1)		
	K_p or $K_{p,C}$	τ_L/τ_W	α (τ_{PD}/τ_P)	K_p or $K_{p,C}$	τ_L/τ_W	α (τ_{PD}/τ_P)
pepR	–	–	–	1.07 ± 0.2	2.4 ± 0.1	–
pepR:ssDNA	0.6 ± 0.2	1.3 ± 0.04	0.52 ± 0.01	1.33 ± 0.3	3.0 ± 0.1	0.62 ± 0.02
pepM	8.2 ± 2.3	1.7 ± 0.02	–	10.2 ± 4.5	1.4 ± 0.02	–
pepM:ssDNA	3.0 ± 1.0	1.8 ± 0.03	0.65 ± 0.01	5.6 ± 1.6	1.9 ± 0.05	0.40 ± 0.01

Partition constants of pepR and pepM, $K_p \pm$ SD, and of their complexes with ssDNA, $K_{p,C} \pm$ SD, were calculated using Eqns (2) and (30), respectively. The ratio between the average lifetime decays in aqueous solution and in lipid (τ_L/τ_w) is also shown, as well as $\alpha = \tau_{\text{Peptide-cargo}}/\tau_{\text{peptide}}$ (Eqn (14)), which refers to the influence of the cargo interaction in pepR or pepM spectroscopic properties. Data are presented as the best-fit value $\pm$ SD.

Journal of PeptideScience

cargo, it is able to interact with zwitterionic POPC membranes. This fact shows that the peptide's molecular rearrangements upon complexation with the ssDNA molecules favor the interaction with lipid membrane, facilitating cellular entry. Our results thus support the idea that studies with free form of CPP are not adequate to conclude on its carrier properties because structural and chemical rearrangements can occur and the CPP affinity and translocation potency may be severely affected or even disrupted [10]. It is worth reminding that the prediction of the membrane partition of these complexes does not directly imply that efficient membrane translocation occurs. A molecular organization of the phospholipids with the CPP–cargo complexes is also needed and may serve as a limiting step for lipid translocation. However, as previously stated by Sargent and co-workers [35] and more recently by our group [13], a lipid membrane process is favored by the increased concentration of the intervenient molecule at the membrane, thus its lipid partition. Taken together, our results reinforce the need for having a tool to determine the interaction of CPP–cargo supramolecular complexes in order to evaluate CPP formulations.

Conclusions

So far, available methodologies could only be used to determine the free CPP partition to membranes; with the methodology presented and applied in this work, it is possible to have direct quantitative data on the partition of CPP–cargo complexes to lipid membranes. It is a very simple tool to compare newly designed and improved CPP as drug carriers and guide drug developers towards CPP optimization in lipid membrane binding. This novel mathematical lipid partition model may serve as a good screening tool and contribute to a more effective and rational design of cellular entry vectors.

Acknowledgements

This work was supported by projects PTDC/QUI/69937/2006 and PTDC/QUI-BIQ/112929/2009 from Fundação para a Ciência e Tecnologia – Ministério da Educação e Ciência (FCT-MEC, Portugal). JMF also acknowledges FCT-MEC for PhD fellowship SFRH/BD/70423/2010. The authors have no competing financial interests.

References

1 Nakase I, Akita H, Kogure K, Gräslund A, Langel Ü, Harashima H, *et al*. Efficient Intracellular Delivery of Nucleic Acid Pharmaceuticals Using Cell-Penetrating Peptides. *Acc. Chem. Res.* 2012; **45**: 1132–1139.
2 Milletti F. Cell-penetrating peptides: classes, origin, and current landscape. *Drug Discov. Today*. 2012; **17**: 850–860.
3 Svensen N, Walton JGA, Bradley M. Peptides for cell-selective drug delivery. *Trends Pharmacol. Sci.* 2012; **33**: 186–192.
4 Timko BP, Whitehead K, Gao W, Kohane DS, Farokhzad O, Anderson D, *et al*. Advances in Drug Delivery. *Annu. Rev. Mater. Res.* 2011; **41**: 1–20.
5 Jarver P, Mäger I, Langel Ü. In vivo biodistribution and efficacy of peptide mediated delivery. *Trends Pharmacol. Sci.* 2010; **31**: 528–535.
6 Bolhassani A. Potential efficacy of cell-penetrating peptides for nucleic acid and drug delivery in cancer. *BBA - Rev. Cancer.* 2011; **1816**: 232–246.
7 Gautam A, Singh H, Tyagi A, Chaudhary K, Kumar R, Kapoor P, *et al*. CPPsite: a curated database of cell penetrating peptides. *Database* 2012; **2012**: bas015–bas015.
8 Heitz F, Morris MC, Divita G. Twenty years of cell-penetrating peptides: from molecular mechanisms to therapeutics. *Brit. J. Pharmacol.* 2009; **157**: 195–206.
9 Green M, Green M, Ishino M, Ishino M, Loewenstein PM, Loewenstein PM. Mutational Analysis of Hiv-1 Tat Minimal Domain Peptides - Identification of Trans-Dominant Mutants That Suppress Hiv-Ltr-Driven Gene-Expression. *Cell* 1989; **58**: 215–223.
10 Fischer R, Fotin-Mleczek M, Hufnagel H, Brock R. Break on through to the Other Side-Biophysics and Cell Biology Shed Light on Cell-Penetrating Peptides. *Chembiochem* 2005; **6**: 2126–2142.
11 Lehto T, Kurrikoff K, Langel Ü. Cell-penetrating peptides for the delivery of nucleic acids. *Expert Opin. Drug Deliv.* 2012; **9**: 823–836.
12 Guterstam P, *et al*. Elucidating cell-penetrating peptide mechanisms of action for membrane interaction, cellular uptake, and translocation utilizing the hydrophobic counter-anion pyrenebutyrate. *Biochim. Biophys. Acta.* 2009; **1788**: 2509–2517.
13 Castanho MARB, Fernandes MX. Lipid membrane-induced optimization for ligand–receptor docking: recent tools and insights for the "membrane catalysis" model. *Eur. Biophys. J.* 2005; **35**: 92–103.
14 Santos N. Quantifying molecular partition into model systems of biomembranes: an emphasis on optical spectroscopic methods. *BBA - Biomembranes* 2003; **1612**: 123–135.
15 Ribeiro M, Melo MN, Serrano ID, Santos NC, Castanho MARB. Drug–lipid interaction evaluation: why a 19th century solution? *Trends Pharmacol. Sci.* 2010; **31**: 449–454.
16 Santos NC, Castanho M. Fluorescence spectroscopy methodologies on the study of proteins and peptides. On the 150th anniversary of protein fluorescence. *Trends App. Spect.* 2002; **4**: 113–125.
17 Markoff L, Falgout B, Chang A. A conserved internal hydrophobic domain mediates the stable membrane integration of the dengue virus capsid protein. *Virology* 1997; **233**: 105–117.
18 Ma L, Jones CT, Groesch TD, Kuhn RJ, Post CB. Solution structure of dengue virus capsid protein reveals another fold. *Proc. Natl. Acad. Sci. U.S.A.* 2004; **101**: 3414–3419.
19 Alves CS, Melo MN, Franquelim HG, Ferre R, Planas M, Feliu L, *et al*. Escherichia coli Cell Surface Perturbation and Disruption Induced by Antimicrobial Peptides BP100 and pepR. *J. Biol. Chem.* 2010; **285**: 27536–27544.
20 Henriques ST, Melo MN, Castanho MARB. Cell-penetrating peptides and antimicrobial peptides: how different are they? *Biochem. J.* 2006; **399**: 1.
21 Splith K, Neundorf I. Antimicrobial peptides with cell-penetrating peptide properties and vice versa. *Eur. Biophys. J.* 2011; **40**: 387–397.
22 Matos PM, Franquelim HG, Castanho MARB, Santos NC. Quantitative assessment of peptide–lipid interactions. *BBA - Biomembranes* 2010; **1798**: 1999–2012.
23 Castanho MA, Prieto MJ. Fluorescence quenching data interpretation in biological systems. The use of microscopic models for data analysis and interpretation of complex systems. *Biochim. Biophys. Acta* 1998; **1373**: 1–16.
24 Nagle JF, Nagle JF, Wiener MC, Wiener MC. Structure of fully hydrated bilayer dispersions. *Biochim. Biophys. Acta* 1988; **942**: 1–10.
25 Ribeiro MMB, Franquelim HG, Castanho MARB, Veiga AS. Molecular interaction studies of peptides using steady-state fluorescence intensity. Static (de)quenching revisited. *J. Pept. Sci.* 2008; **14**: 401–406.
26 Veiga S, Yuan Y, Li X, Santos NC, Liu G, Castanho MARB. Why are HIV-1 fusion inhibitors not effective against SARS-CoV? Biophysical evaluation of molecular interactions. *BBA - Gen. Subjects.* 2006; **1760**: 55–61.
27 Fields GB, Fields GB, Noble RL, Noble RL. Solid phase peptide synthesis utilizing 9-fluorenylmethoxycarbonyl amino acids. *Int. J. Pept. Protein Res.* 1990; **35**: 161–214.
28 (n.d.).
29 Provencher SW. CONTIN: a general purpose constrained regularization program for inverting noisy linear algebraic and integral equations. *Comput. Phys. Commun.* 1982; **27**: 229–242.
30 Provencher SW, Provencher SW. A constrained regularization method for inverting data represented by linear algebraic or integral equations. *Comput. Phys. Commun.* 1982; **27**: 213–227.
31 Santos NC, Castanho MA. Teaching light scattering spectroscopy: the dimension and shape of tobacco mosaic virus. *Biophys. J.* 1996; **71**: 1641–1650.
32 Domingues MM, Santiago PS, Castanho MARB, Santos NC. What can light scattering spectroscopy do for membrane-active peptide studies? *J. Pept. Sci.* 2008; **14**: 394–400.
33 Lakowicz JR. *Principles of Fluorescence Spectroscopy*. Springer: Berlin, 2006.
34 Ladokhin AS, Jayasinghe S, White SH. How to Measure and Analyze Tryptophan Fluorescence in Membranes Properly, and Why Bother? *Anal. Biochem.* 2000; **285**: 235–245.
35 Sargent DF, Schwyzer R. Membrane lipid phase as catalyst for peptide-receptor interactions. *Proc. Natl. Acad. Sci. U.S.A.* 1986; **83**: 5774–5778.
36 Rohacova J, Marin ML, Miranda MA. Complexes between Fluorescent Cholic Acid Derivatives and Human Serum Albumin. A Photophysical Approach To Investigate the Binding Behavior. *J. Phys. Chem. B* 2010; **114**: 4710–4716.

